2022 7th International Conference on Electric Vehicular Technology (ICEVT)
September 14-16, Bali, Indonesia

2022 7th International Conference on Electric Vehicular Technology (ICEVT) | 978-1-6654-0942-1/22/$31.00 ©2022 IEEE | DOI: 10.1109/ICEVT55516.2022.9925018

Optimal Gantry Crane PID Controller Based on LQR With Prescribed Degree of Stability by Means of GA, PSO, and SA

Steven Bandong
Engineering Physics Doctoral Program, Faculty of Industrial Technology
Institut Teknologi Bandung
Bandung, Indonesia
bandong.steven@gmail.com

Rizky Cahya Kirana
Instrumentation and Control Graduate Program
Institut Teknologi Bandung
National Center for Sustainable Transportation Technology
Bandung, Indonesia
rizkycahyakirana@gmail.com

Yul Yunazwin Nazaruddin
Instrumentation and Control Research Group, Department of Engineering Physics
Institut Teknologi Bandung
National Center for Sustainable Transportation Technology
Bandung, Indonesia
yul@tf.itb.ac.id

Endra Joelianto
Instrumentation and Control Research Group, Department of Engineering Physics
Institut Teknologi Bandung
National Center for Sustainable Transportation Technology
Bandung, Indonesia
ejoel@tf.itb.ac.id

***Abstract*—Trade between islands and countries is increasing in the current era of globalization which also increases the traffic of goods at ports. Rubber Tyred Gantry Crane (RTGC) is an important component in the seaports distribution chain, which act as a loading and unloading machine at the container yard. However, heavy trade traffic will likely cause fatigue and negligence if the RTGC is operated manually. Therefore, it is necessary to automate RTGC by applying optimal control. The paper introduces an alternative approach to designing an optimal PID controller built from the LQR method combined with a prescribed degree of stability for achieving the required transient and steady-state responses of RTGC in the port. Genetic Algorithm (GA), Particle Swarm Optimization (PSO), and Simulated Annealing (SA) are applied to select the suitable stability degree value and weighting matrices in the LQR cost function. Simulation results indicate that GA can provide the optimal PID controller to follow the reference trajectory and minimize the swing angle better than PSO and SA.**

Keywords—RTGC, PID, LQR, Prescribed Degree Stability, Particle Swarm Optimization, Simulated Annealing, Genetic Algorithm

I. INTRODUCTION

Control problems in the gantry crane system can be divided into two categories: controlling the trolley's position and the container's sway angle. Position control attempts to move the trolley to the desired position based on the desired trajectory or with the least amount of position error in its final state. Sway angle control attempts to reduce container swing at the desired position [1].

The PID controller was chosen because it has a large number of implementations in many control systems, making it a robust controller [2]. PID has been widely used as a controller in various applications, such as controlling wind turbines [3], electric motors [4], and controlling the temperature in boilers [5]. This paper modeled the gantry crane system with two degrees of freedom to keep the complexity low while improving the PID controller. A PID controller is used for position control, and another PID controller is used for sway angle control. To achieve optimal control stability and performance, the parameters of the PID controllers must be suitably selected through tuning. Particle Swarm Optimization (PSO), Simulated Annealing (SA), and Genetic Algorithm (GA) are the three optimization techniques used in the tuning process.

PSO, SA, and GA are metaheuristic methods used to improve the 2D Ball Balancer Arrangement solution through each optimization iteration in which the cost function is minimized with the objectives of delay time, rise time, and settling time [6]. A hybrid SA-GA is used to optimize the automatic generation control of power systems [7], job scheduling problems [8], and brain tumor classification & segmentation [9]. PSO is commonly used to control DC motors [10].

The controller should be optimized in gantry crane automation to produce an accurate movement with low sway. [11] discusses how to design an anti-swing gantry crane control robust feedback controller using metaheuristic optimization techniques for single-objective restricted optimization. [12] describes an adaptive integral sliding mode control (AISMC) method for 4-DOF tower cranes with payload sway reduction; the integral sliding mode control provides robust behavior, the adaptive control provides adaptive performance, and the swing-damping term is added to suppress and eliminate payload swing angles. Even when frictions are erroneously corrected, stable errors can be successfully decreased; hence positioning accuracy can be increased [13]. In [14], PSO, SFS, and FPA were used to optimize the performance of the PID controller for position and sway control.

LQR offers an optimal control method that allows the weighting of the matrix Q for state and R for controller output. It allows the minimization of control errors and optimization of controller output energy. However, LQR is a full state feedback regulator which requires measurement or estimation of the entire state system. This paper investigates the conversion of LQR to PID controller by considering the

stability degree for the position controller and sway angle reduction. It starts from LQR synthesis and improves the stability by the degree of stability (α) to find the optimal PID controller. PSO, SA, and GA were applied to select the appropriate α value and LQR parameters following the desired trajectory.

II. RTGC Control Model

The 2D Gantry Crane system can be depicted in Fig. 1. m_2 is the mass of the trolley. F is the driving force of the trolley by the DC motor. g is the force of gravity, l the length of the rope, x the position of the trolley, θ is the angle of swing, and m_1 is the mass of the load, which in this case is a container. m_1 has kinetic energy (T_1) and Potential Energy (P_1)

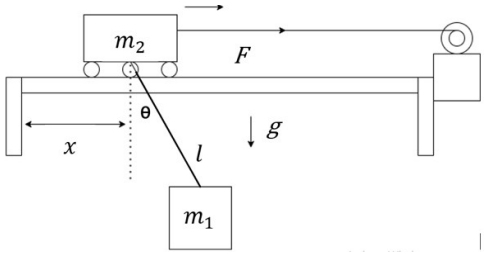

Fig. 1. 2D gantry crane representation.

$$T_1 = \frac{1}{2} m_1 \left(\dot{x}^2 + l^2 \dot{\theta}^2 + 2\dot{x} l \dot{\theta} \cos\theta \right) \quad (1)$$

$$P_1 = -m_1 g l \cos\theta \quad (2)$$

assuming the position of the trolley as a reference, m_2 has zero potential energy (P_2 =0) and its kinetic energy is

$$T_2 = \frac{1}{2} m_2 \dot{x}^2 \quad (3)$$

(1), (2), and (3) are substituted into (4) to obtain L which will be substituted in the Lagrange equation (5):

$$L = T - P \quad (4)$$

$$L = \frac{1}{2} m_1 \left(\dot{x}^2 + l^2 \dot{\theta}^2 + 2\dot{x} l \dot{\theta} \cos\theta \right) + \frac{1}{2} m_2 \dot{x}^2 + m_1 g l \cos\theta \quad (5)$$

$$\frac{d}{dt}\left(\frac{\partial L}{\partial q_i} \right) - \frac{\partial L}{\partial q_i} = Q_i \quad (6)$$

Substitution of L in (6) will result in the dynamic equation of the 2D RTGC model:

$$(m_1 + m_2)\ddot{x} + m_1 l \ddot{\theta} \cos\theta - m_1 l \dot{\theta}^2 \sin\theta + D\dot{x} = F \quad (7)$$

$$m_1 l^2 \ddot{\theta} + m_1 l \ddot{x} \cos\theta + m_1 \dot{x} l \dot{\theta} \sin\theta + m_1 g l \sin\theta = 0 \quad (8)$$

RTGC dynamic models (7) and (8) are integrated with the motor model (9) to obtain a complete RTGC model. Details of getting the motor model can be seen in [14].

$$V = \left(\frac{R.r_p}{K_t.r} \right) F + \frac{K_e.r}{r_p} \dot{x} \quad (9)$$

Substituting (7) to (9) to obtain a nonlinear RTGC model driven by a DC motor:

$$V = \left(\frac{R.r_p}{K_t.r} \right)(m_1 + m_2)\ddot{x} + \left(\frac{D.R.r_p}{K_t.R} + \frac{K_e.r}{r_p} \right)\dot{x} + \left(\frac{m_1 l.R.r_p}{K_t.r} \right) \left(\ddot{\theta}\cos\theta - \dot{\theta}^2 \sin\theta \right) \quad (10)$$

$$l^2 \ddot{\theta} + l\ddot{x}\cos\theta + gl\sin\theta = 0 \quad (11)$$

For computational and simulation needs, (10) and (11) are linearized using the assumption of a small angle ($\theta \approx 0$), and $\sin\theta \approx \theta$, $\cos\theta \approx 1$, and $\dot{\theta}^2 \approx 0$. (12) and (13) are equations of the RTGC system and its driving motor after linearization.

$$V = \left(\frac{R.r_p}{K_t.r} \right)(m_1 + m_2)\ddot{x} + \left(\frac{D.R.r_p}{K_t.R} + \frac{K_e.r}{r_p} \right)\dot{x} + \left(\frac{m_1 l.R.r_p}{K_t.r} \right)\ddot{\theta} \quad (12)$$

$$l^2 \ddot{\theta} + l\ddot{x} + gl\theta = 0 \quad (13)$$

III. LQR with a Prescribed Degree of Stability

A closed-loop system with a defined degree of stability alpha may be constructed using LQR theory and the proper time-varying choices of Q and R [15]. Consider the performance indicator

$$V = \int_0^\infty e^{2\alpha t} \left(x^T \overline{Q} x + u^T \overline{R} u \right) dt \quad (14)$$

where $\overline{Q}$ and $\overline{R}$ are constants matrices. Variables $\eta(t) = e^{\alpha t} x(t)$ and $v(t) = e^{\alpha t}\,\mathrm{u}(t)$ are introduced, then the state equation $\dot{x} = Ax + Bu$ becomes

$$\dot{\eta} = (A + \alpha I)\eta + Bv \quad (15)$$

and the performance index becomes

$$V = \int_0^\infty \left(\eta^T \overline{Q} \eta + v^T \overline{R} v \right) dt \quad (16)$$

The constant LQR problem given by (15) and (16) will result in an asymptotically stable $\eta(t)$ and since $\mathrm{x}(t) = e^{-\alpha t}\eta(t)$, $\mathrm{x}(t)$ must be asymptotically stable with a stability degree equal too $-\alpha$. Thus, to design for a degree of stability, all that is required is to solve the modified ARE.

$$0 = (A + \alpha I)^T \overline{P} + \overline{P}(A + \alpha I) + \overline{Q} - \overline{P} B \overline{R}^{-1} B^T \overline{P} \quad (17)$$

and use

$$u^*(t) = -\overline{R}^{-1} B^T \overline{P} x(t) \quad (18)$$

IV. Full State Feedback Representation

Assume a linear time-invariant plant with a single input and output and characterized by a linear system with state space representation.

$$\dot{x}(t) = Ax(t) + B_1 u(t); \qquad x(0) = 0 \qquad (19)$$

$$y(t) = Cx(t)$$

where x is the solution of (19), u is supposed to represent the output of a PID controller with input y, and the PID form is then employed

$$u(t) = K_1 \int_0^t y(t)dt + K_2\, y(t) + K_3 \frac{dy(t)}{dt} \qquad (20)$$

where $K_1 = \frac{K_p}{T_i}$, $K_2 = K_p$, and $K_3 = K_p T_d$. K_p, T_i and T_d denote proportional gain, time integral, and time derivative of the PID controller.

The control law (20) is stated as a state feedback law [16] and from (19) gives the following representation

$$y = Cx$$
$$\dot{y} = CAx + CB_2 u$$
$$\ddot{y} = CA^2 x + CAB_1 u + CB_2 \dot{u} \qquad (21)$$

Based on (21), the representation (20) becomes (22). (23) gives the value $\hat{K}$ so that the control law is obtained as in (19).

$$\left(1 - K_3 CB_2\right)\dot{u} - \left(K_3 CA^2 + K_2 CA + K_1 C\right)x - \left(K_3 CAB_2 + K_2 CB_2\right)u = 0 \qquad (22)$$

$$\hat{K}^T = \begin{bmatrix} \hat{K}_1 \\ \hat{K}_2 \\ \hat{K}_3 \end{bmatrix} = \left(1 - K_3 CB_2\right)^{-1} \begin{bmatrix} K_1 \\ K_2 \\ K_3 \end{bmatrix} \qquad (23)$$

$$\dot{u} = \hat{K}^T \begin{bmatrix} C^T \\ A^T C^T \\ \left(A^2\right)^T \end{bmatrix} x + \hat{K}^T \begin{bmatrix} 0 \\ B_2^T C^T \\ B_2^T A^T C^T \end{bmatrix} u \qquad (24)$$

Equation (24) is written in a simpler form as follows

$$u_a = K_a x_a(t) \qquad (25)$$

where

$$u_a(t) = \dot{u}(t), \quad x_a(t) = \begin{bmatrix} x(t) & u(t) \end{bmatrix}^T$$

$$K_a = \begin{bmatrix} C^T & A^T C^T & \left(A^2\right)^T \\ 0 & B_2^T C^T & B_2^T A^T C^T \end{bmatrix} \hat{K} = \Gamma \hat{K} \qquad (26)$$

$x_a(t)$ is the augmentation state associated with the following system augmentation

$$\dot{x}_a(t) = A_a x_a(t) + B_a u_a(t) \qquad (27)$$

where,

$$A_a = \begin{bmatrix} A & B_2 \\ 0 & 1 \end{bmatrix}; \qquad B_a = \begin{bmatrix} 0 \\ 1 \end{bmatrix} \qquad (28)$$

The detailed derivation of this method can be seen in [15], [17].

V. Methods and Experiments

The proposed swing angle and position control system is designed as shown in Fig. 4. The control system is developed to be able to follow the position trajectory designed based on the ITAE order 3 performance criteria as in (29)

$$X_{ref} = \frac{\omega^3}{s^3 + 1.75\omega s^2 + 2.15\omega^2 s + 1.5\omega^3} \qquad (29)$$

the appropriate value of w is selected to obtain a settling time of 4.24 s and a rise time of 2.6 s. A clearer picture of the desired reference trajectory can be seen in Fig. 2.

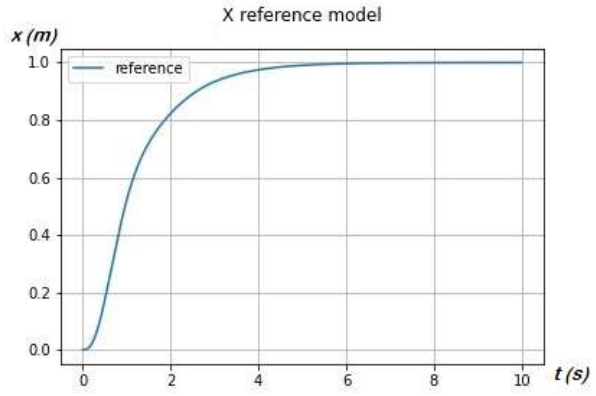

Fig. 2. Position-shift trajectory reference.

Finding the optimal controller parameters is necessary to achieve minimal positional error or follow the reference trajectory well. In this paper, 2 PID controllers are used, one controller as a position controller and the other as a swing angle PID controller. The PID parameter value is obtained using the optimal LQR accompanied by the prescribed degree of stability.

The LQR parameters in the form of matrix Q and R and the prescribed degree of stability (a) parameters are optimized using PSO, SA, and GA to obtain an optimal controller that can follow the trajectories reference. The ITSE cost function is used to measure the error against the reference trajectory and becomes an objective of optimization performance, as stated in (30)

$$J = \int_{t_0}^{t_1} t\left(x - x_{ref}\right)^2 dt + \int_{t_1}^{t_{end}} t\left(\theta\right)^2 dt + \int_{t_2}^{t_{end}} t\left(x - x_{ref}\right)^2 dt \qquad (30)$$

where t_0 (0s) is the initial simulation time, t_1 (2.6s) is the rise time, and t_2 (4.24s) is the settling time of the reference trajectory. t_{end} is the final simulation time, in this case, 10 s. x is the output of the controlled position, x_{ref} is the reference trajectory in Fig. 2, and θ is the sway angle.

The optimal controller is designed following the flow diagram in Fig. 3. The RTGC model in (12) and (13) are made using the prototype RTGC parameters in TABLE I. The results of the initial generation or the results of the updated solutions Q, R, and α from PSO, SA, and GA are used to find

potential PID parameters. From the solution of the Algebraic Ricatti Equation (ARE) on (17), can be calculated $\hat{K}$ using (26). Then the PID constant can be found by solving (23). The J cost function is calculated to assess whether the solution is optimal; then, if it is not optimal, the values of Q, R, and α are updated based on the PSO, SA, and GA algorithms.

TABLE I. RTGC MODEL PARAMETER

Parameter	Value	Unit	Parameter	Value	Unit
m_1	1	Kg	R	0,5	Ω
m_2	1,5	Kg	K_t	0,0071619	NM / A
l	0,5	m	K_e	0,0071619	Vs / rad
g	9,81	m/s^2	r_p	0,012	m
D	12,32	Ns/m	r	1	-

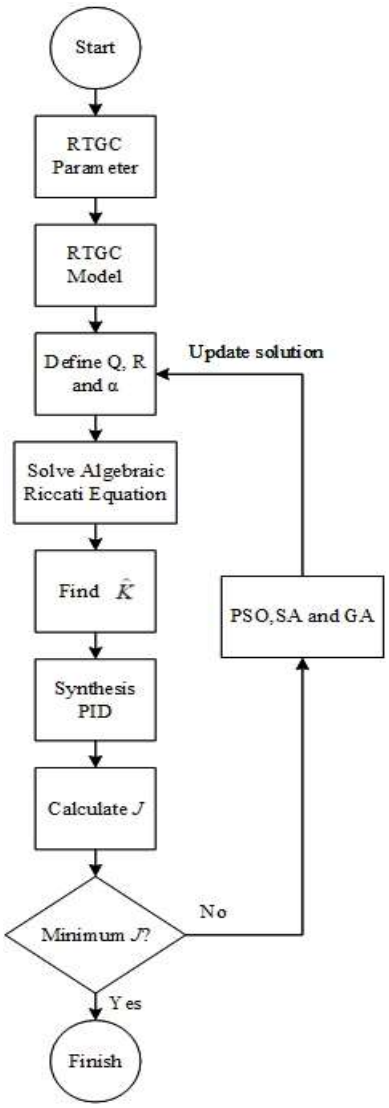

Fig. 3. Optimization Q, R, and α flow diagram.

VI. RESULTS AND DISCUSSIONS

The optimization results of parameters Q, R, and α can be seen in TABLE II. The optimal parameters are then used to find the PID parameters for the position and sway angle controller, as shown in TABLE III. Based on the cost function J value, PSO and GA give the smallest error value, followed by SA.

TABLE II. Q, R, AND A OPTIMIZATION RESULTS

Parameters	Optimization Range	Optimization Results		
		PSO	*SA*	*GA*
Q [1]	50-1000	50	127.13	51.90
Q [2]	50-1000	50	307.09	90.87
Q [3]	50-1000	50	76.77	234.87
Q [4]	50-1000	50	99.88	50.50
Q [5]	50-1000	999.96	309.36	951.48
R	50-1000	7.37	817.84	999.87
α	2-10	0.70	7.35	7.34

TABLE III. PID SYNTHESIS RESULT

Objective	Controller	PSO	SA	GA
Position	K_p	9130	9030	8980
	K_i	23000	22700	22500
	K_d	234	235	239
Sway	K_p	3520	3470	3450
	K_i	-27.9	-28.2	-28.6
	K_d	81.3	82.4	84
J		0.0020509	0.0020510	0.0020509

The obtained value of J of the optimization results is very small for the three optimization methods. The maximum J value is the result of SA optimization, 0.0020510, which gives the worst result of these controller optimizations. This result can be confirmed in Fig. 5, where the movement of the trolley position followed the desired trajectory. Fig. 5 (left) shows that the position response of the PSO optimization results has followed the same trajectory as the GA and SA control results. The results of the swing angle control, Fig. 5 (center), also show that PSO, SA, and GA have nearly the same control result. They gave nearly the same PID parameter (see TABLE III), and the control result in terms of position and sway control gave similar responses (see Fig. 5). It is confirmed by the J value, which only slightly differs where PSO is better than GA and SA (see Fig. 6).

In Fig. 5 (left), the control results still have errors at 0-4 s. In this period, the trolley begins to move rapidly to reach 1 meter. Because of this fast-moving, the control results make errors and appear to oscillate around the trajectory at 0-4s seconds; especially at 1.5-3s, the oscillations are seen more clearly. It is because the trolley moves at a higher speed initially but is forced to slow down as it approaches the target position (1m), and the trolley adjusts to the new speed. In the 4-10s period, the position error is very small because the portion of the error in the 4.24-10 s period is larger according to equation J (eq. 30); therefore, the optimization algorithm tends to be stronger in minimizing errors in that time range.

However, this is under the desired result, which focuses on minimizing error at the end position of the trolley.

In Fig. 5 (center), due to the fast displacement at the beginning, there will be large oscillations for the 0-4s period. It can be seen in the position trajectory, which has a steeper slope in this period, so the desired speed is also high at the beginning. In addition, according to the cost function J (eq 30) in the 0-2.6s period, the control focuses more on achieving the desired position trajectory. In the period of 2.6-10 s then, the damping of the swing angle is active (eq.30), and the swing angle confirms that the controller reduces from 2.6-10s. The achievable control signal is also presented in Fig. 5 (right), and PSO, SA, and GA give almost similar results; therefore, these methods' position and sway response only have a slight difference.

A detailed description of the control performance is also shown in TABLE IV. Rise time, settling time, overshoot, and average steady-state error are used to measure position controller performance. Settling time, maximum amplitude, minimum amplitude, and average steady-state error are used to measure the sway control performance. GA provides the best performance because it excels in faster rise time, settling time, and a slight error difference with PSO in position control. The PSO sway control also provides the smallest settling time value, maximum amplitude, and average steady-state error. The performance of the three optimization methods in parameter search is also presented in Fig. 6.

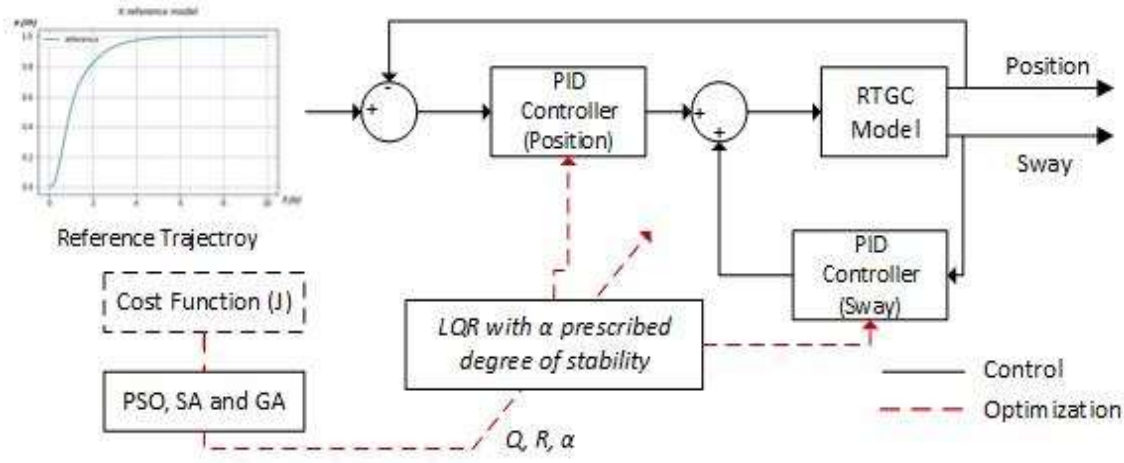

Fig. 4. The proposed control system design.

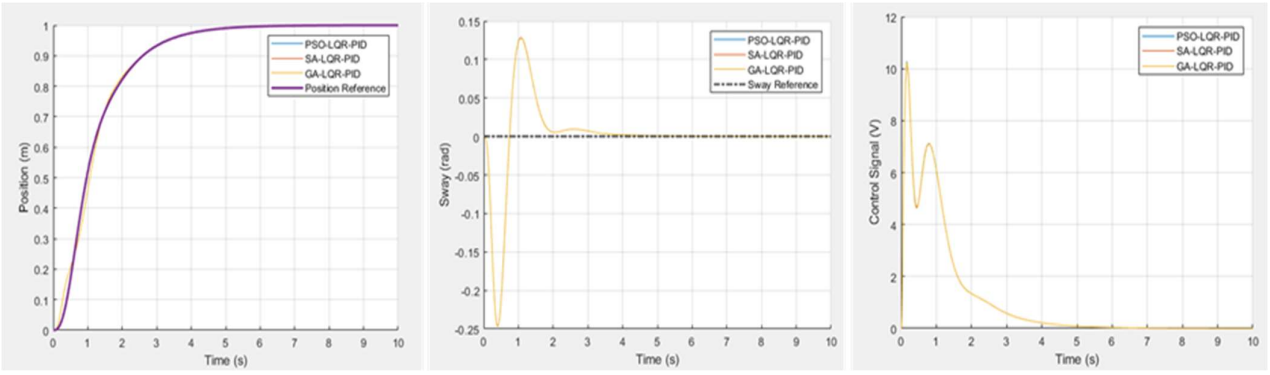

Fig. 5. Comparison of position (left), sway angle (center), and control signal (right).

TABLE IV. CONTROL PERFORMANCE METRICS

Method	Position				Sway			
	Rise Time (s)	*Settling Time (s)*	*Overshoot (m)*	*Average SSE (m)*	*Settling Time (s)*	*Max Amplitude (rad)*	*Min Amplitude (rad)*	*Average SSE (rad)*
PSO	2.58262	4.22332	0	0.00008	**4.12169**	**0.12789**	-0.24674	**0.00036**
SA	2.58266	4.22333	0	0.00008	4.12193	0.12837	**-0.24649**	**0.00036**
GA	**2.58246**	**4.22322**	0	0.00008	4.12172	0.12796	-0.24669	**0.00036**

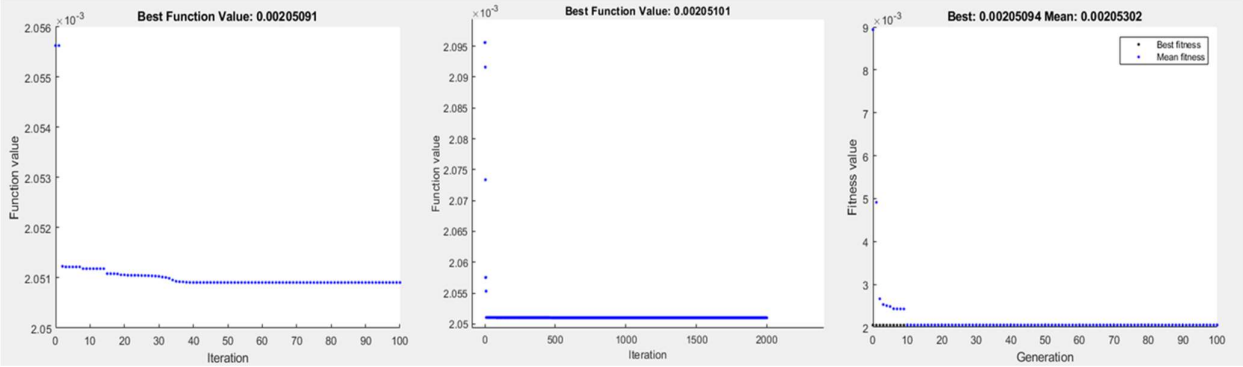

a. PSO-LQR-PID b. SA-LQR-PID c. GA-LQR-PID

Fig. 6. PSO, SA, and GA optimization performance.

VII. Conclusion

This paper designed an alternative optimal PID control system based on LQR and prescribed degree of stability α to find the optimal gantry crane PID controller. PSO, SA, and GA were used as optimization tools, and the optimal PID parameters were obtained to follow the container transfer trajectory and minimize the container sway angle. PSO and GA provided better position and swing angle control performance than SA in settling time, rise time, minimizing maximum sway angle, and average steady-state error. Future research will design a robust RTGC control system against changes in container mass and the length of the container carrier rope. The designed control system will be applied to the RTGC prototype on a laboratory scale.

Acknowledgment

This work was supported Doctoral Dissertation Research Scholarship 2022 from the Ministry of Education, Culture, Research, and Technology Indonesia. S. Bandong is supported by the Indonesia Endowment Fund for Education (LPDP), Indonesia

References

[1] M. S. Korytov, V. S. Shcherbakov, and V. v. Titenko, "Effect of the payload mass on forces acting from the overhead crane drives during movement in the mode of suppressing uncontrolled oscillations," *J Phys Conf Ser*, vol. 1546, no. 1, p. 012134, May 2020.

[2] R. P. Borase, D. K. Maghade, S. Y. Sondkar, and S. N. Pawar, "A review of PID control, tuning methods and applications," *Int J Dyn Control*, vol. 9, no. 2, pp. 818–827, Jul. 2020.

[3] A. Gambier and Y. Y. Nazaruddin, "Collective Pitch Control with Active Tower Damping of a Wind Turbine by Using a Nonlinear PID Approach," *IFAC-PapersOnLine*, vol. 51, no. 4, pp. 238–243, Jan. 2018.

[4] A. Kholid, R. A. Fauzi, Y. Yunazwin Nazaruddin, and E. Joelianto, "Power Optimization of Electric Motor using PID-Fuzzy Logic Controller," *ICEVT 2019 - Proceeding: 6th International Conference on Electric Vehicular Technology 2019*, pp. 189–195, Nov. 2019.

[5] Y. Y. Nazaruddin, A. N. Azi, and O. Priatna, "Improving performance of PID controller using artificial neural network for disturbance rejection of high pressure steam temperature control iiflndustrial boiler," *2008 International Conference on Control, Automation and Systems, ICCAS 2008*, pp. 1204–1207, 2008.

[6] A. Surana and B. Bhushan, "Design and Comparison of PSO, SA and GA tuned PID Controller for Ball Balancer Arrangement," *2021 4th International Conference on Electrical, Computer and Communication Technologies, ICECCT 2021*, 2021.

[7] A. Tabak and İ. İlhan, "An effective method based on simulated annealing for automatic generation control of power systems," *Appl Soft Comput*, vol. 126, Sep. 2022.

[8] B. KARİMA and Z. OUARDA, "Hybrid Metaheuristic for Optimization Job-Shop Scheduling Problem," *International Journal of Informatics and Applied Mathematics*, vol. 1, no. 1, pp. 1–9, Dec. 2018, Accessed: Oct. 08, 2022.

[9] A. KHARRAT and M. NEJI, "Feature selection based on hybrid optimization for magnetic resonance imaging brain tumor classification and segmentation," *Appl Med Inform*, vol. 41, no. 1, pp. 9–23, Mar. 2019, Accessed: Oct. 08, 2022.

[10] E. S. Rahayu, A. Ma'arif, and A. Çakan, "Particle Swarm Optimization (PSO) Tuning of PID Control on DC Motor," *International Journal of Robotics and Control Systems*, vol. 2, no. 2, pp. 435–447, Jul. 2022.

[11] M. I. Solihin, W. H. Lim, S. S. Tiang, and C. K. Ang, "Modified particle swarm optimization for robust anti-swing gantry crane controller tuning," *Lecture Notes in Electrical Engineering*, vol. 666, pp. 1173–1192, 2021.

[12] M. Zhang, Y. Zhang, H. Ouyang, C. Ma, and X. Cheng, "Adaptive integral sliding mode control with payload sway reduction for 4-DOF tower crane systems," *Nonlinear Dyn*, vol. 99, no. 4, pp. 2727–2741, Mar. 2020.

[13] N. Sun, Y. Wu, H. Chen, and Y. Fang, "Antiswing Cargo Transportation of Underactuated Tower Crane Systems by a Nonlinear Controller Embedded With an Integral Term," *IEEE Transactions on Automation Science and Engineering*, vol. 16, no. 3, pp. 1387–1398, Jul. 2019.

[14] S. Bandong, M. R. Miransyahputra, Y. Setiaji, Y. Y. Nazaruddin, P. I. Siregar, and E. Joelianto, "Optimization of Gantry Crane PID Controller Based on PSO, SFS, and FPA," in 2021 60th Annual Conference of the Society of Instrument and Control Engineers of Japan, pp. 338–343, 2021.

[15] E. Joelianto, "Linear Quadratic Control: A State Space Approach," *ITB Press Bandung*, 2017.

[16] D. Williamson and J. B. Moore, "Three-Term Controller Parameter Selection Using Suboptimal Regulator Theory," *IEEE Trans Automat Contr*, vol. 16, no. 1, pp. 82–83, 1971.

[17] E. Joelianto and Tommy, "A robust DC-to-DC buckboost converter using PID hoo-backstepping controller," *Proceedings of the International Conference on Power Electronics and Drive Systems*, vol. 1, pp. 591–594, 2003.

[18]